Anomalous Magnetic Behavior in Three Kinds of 3-(Aryl-substituted)-1,5-diphenylverdazyl Radical Crystals (*p*-FPDV, *p*-PyDV and *m*-PyDV) Induced by Frustrated Spin Interaction

K. Mukai,*,† M. Matsubara,† H. Hisatou,† Y. Hosokoshi,‡ K. Inoue,‡ and N. Azuma†

Department of Chemistry, Faculty of Science, Ehime University, Matsuyama 790-8577, Japan, and Institute for Molecular Science, Myodaiji, Okazaki 444-8585, Japan

Received: March 25, 2002; In Final Form: June 10, 2002

Magnetic susceptibilities (χ_M) of three kinds of 3-(aryl-substituted)-1,5-diphenyl-verdazyl radical crystals (aryl: 4-fluorophenyl (*p*-FPDV), 4-pyridyl (*p*-PyDV), and 3-pyridyl (*m*-PyDV)) have been measured between 1.8 and 300 K, showing a broad maximum T_{max} at 200, 272, and 157 K, respectively. The values of T_{max} observed are 1 or 2 orders of magnitude larger than those for usual organic neutral radical crystals, suggesting strong intermolecular antiferromagnetic (AFM) exchange interactions (J) in the crystals. The temperature dependence of the susceptibilities cannot be explained by a simple model, such as the one-dimensional (1D) Heisenberg AFM linear- and alternating-chain model. The values of χ_M observed for the *p*-FPDV, *p*-PyDV, and *m*-PyDV radicals are about 42, 76, and 35% larger than the corresponding values calculated by a 1D Heisenberg AFM linear-chain model at each temperature. The result of the crystal structure analysis of *p*-FPDV indicates the existence of butterfly-type spin frustration in the system. The origin of the anomalous magnetic behavior observed for these verdazyl radical crystals has been discussed based on the results of the crystal structure analysis and unpaired spin density calculation.

1. Introduction

The study of magnetic property of organic radical crystals has attracted much attention since the finding of the first organic ferromagnet, *p*-nitrophenyl nitronyl nitroxide (β-phase) (T_C = 0.60 K), in 1991.[1−3] Verdazyl radicals are well known as one of the representative stable neutral free radicals. Recently, the magnetic properties of these verdazyl radical crystals have been studied extensively.[4−16] These verdazyl radicals are aromatic compounds with a delocalized π-electron system and with planar molecular structure,[4,12,16−18] and generally show magnetic property that can be explained by one-dimensional (1D) Heisenberg antiferromagnetic (AFM) linear- or alternating-chain model.[4,7,10,12,14−16] At low-temperature region, the verdazyl radical crystals show several interesting magnetic properties such as ferromagnetism,[9,10] weak ferromagnetism,[5,6,11,13] antiferromagnetism,[12] and spin-Peierls transition.[15] Further, the intermolecular ferromagnetic (FM) exchange interaction was observed for these verdazyl radicals with high probability, because of a very strong spin polarization effect in them.[14]

Recently, we prepared the (1:2) salts of *p*- and *m*-ethylpyridinium-substituted verdazyl radical cation with tetracyanoquinodimethane (TCNQ) anion, and found that the salts are pure organic magnetic semiconductors.[19] Nakatsuji et al.[20] prepared the charge transfer (CT) complexes of the verdazyl radicals with 2,3,5,6-tetrafluoro-7,7,8,8-tetracyanoquinodimethane ($TCNQF_4$) and 2,3-dichloro-5,6-dicyano-1,4-benzoquinone (DDQ) and studied the magnetic properties of the complexes. Further, the magnetic properties of the transition metal complexes of the verdazyl radicals have been investigated by Brook et al.[21,22] and Hicks et al.[23]

In the present work, we prepared 3-(4-fluorophenyl)-1,5-diphenylverdazyl (*p*-FPDV), 3-(4-pyridyl)-1,5-diphenylverdazyl (*p*-PyDV), and 3-(3-pyridyl)-1,5-diphenylverdazyl (*m*-PyDV) radicals (see Scheme 1) and studied the magnetic properties of these radical crystals. The *p*- and *m*-PyDV radicals were used as precursors of the *p*- and *m*-ethyl-pyridinium-substituted verdazyl radical cations, which are the donor components of the above organic magnetic semiconductors. The magnetic susceptibilities of *p*-FPDV, *p*-PyDV, and *m*-PyDV show a broad maximum at T_{max} = 200, 272, and 157 K, respectively, suggesting strong intermolecular AFM exchange interaction in these radical crystals.[16] However, the susceptibilities of these radical crystals cannot be explained by simple 1D Heisenberg AFM linear- and alternating-chain models, which are generally used for the analyses of magnetic properties of organic free radical crystals. The result of the crystal structure analysis of *p*-FPDV indicated the existence of geometrical spin frustration in the system. Spin frustration is one of the interesting magnetic behaviors.[24] However, the examples of organic free radical crystals with frustrated spin interaction are very limited.[25−28] We report here a new spin-frustrated system found for the *p*-FPDV radical crystal.

SCHEME 1

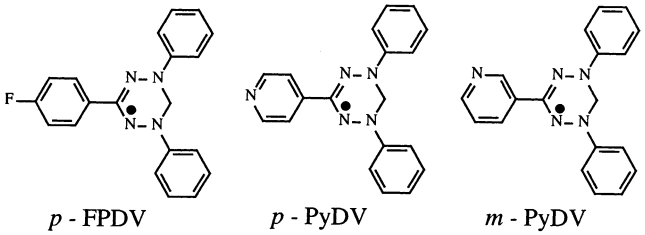

p - FPDV *p* - PyDV *m* - PyDV

2. Experimental Section

2.1. Synthesis. *p*-FPDV, *p*-PyDV, and *m*-PyDV radical crystals were prepared according to a procedure similar to that used by Kuhn et al.[29] to prepare a 1,3,5-triphenylverdazyl (TPV) radical.

* Corresponding author. Tel.: 81-89-927-9588; Fax.: 81-89-927-9590. E-mail: mukai@chem.sci.ehime-u.ac.jp

† Ehime University.

‡ Institute for Molecular Science.

10.1021/jp020801j CCC: $22.00
Published on Web 08/06/2002

3-(4-Fluorophenyl)-1,5-diphenylverdazyl Radical (*p*-FPDV). To a stirred solution of 3-(4-fluorophenyl)-1,5-diphenylformazan[29] (3.20 g, 10.1 mmol) in dimethylformamide (160 mL) at 20 °C, formalin (11.0 mL) was added slowly, and stirring was continued for 30 min. To this a 2 M NaOH solution (23.0 mL) was added slowly, and the reaction was continued for 2 h. The color of the solution changed from purple to green. Then the mixture was poured into water. The green products precipitated were filtered and washed with water and then with a small quantity of methanol. Recrystallization from acetone−ethanol (1:1, v/v) solution afforded the deep green prismatic crystals (1.30 g, 39%): mp 151.5−153.5 °C; UV (ethanol) λ_{max} (log ϵ) 715 (3.43), 396 (3.72), 272 (4.36), 252 (4.31). Found: C, 71.92; H, 4.91; N, 17.47%. Calcd for $C_{20}H_{16}N_4F$: C, 72.49; H, 4.87; N, 16.91%.

The *p*-PyDV and *m*-PyDV were prepared similarly.

3-(4-Pyridyl)-1,5-diphenylverdazyl Radical (*p*-PyDV). Recrystallization from ethanol solution afforded the thin green needle crystals: mp 165.0−166.5 °C; UV (ethanol) λ_{max} (log ϵ) 710.5 (3.61), 459.0 (3.92), 238.5 (4.42). Found: C, 72.67; H, 5.27; N, 22.40%. Calcd for $C_{19}H_{16}N_5$: C, 72.59; H, 5.13; N, 22.28%.

3-(3-Pyridyl)-1,5-diphenylverdazyl Radical (*m*-PyDV). Recrystallization from ethanol solution afforded the green powder crystals: mp 151.0−152.0 °C; UV (ethanol) λ_{max} (log ϵ) 713.0 (3.61), 441.0 (3.86), 304.5 (4.31), 282.0 (4.29). Found: C, 72.76; H, 5.26; N, 22.36%. Calcd for $C_{19}H_{16}N_5$: C, 72.59; H, 5.13; N, 22.28%.

2.2. Crystal Data and Structure Determination. The lattice parameters for *p*-FPDV were obtained at 25 °C on a Rigaku AFC5R four-circle diffractometer angles for 25 automatically centered reflections in the range $47.8° \leq 2\theta \leq 52.0°$, using graphite-monochromatized Cu−Kα radication ($\lambda = 1.54178$ Å) from a 12 kW type rotating-anode generator equipped with a fine-focus anode. The intensity data were collected on the same diffractometer and at the same temperature. The $\omega - 2\theta$ scan mode with a scan rate of 16° min^{-1} (in ω) was applied for 1539 unique reflections, giving 999 with $I \geq 2.50\sigma(I)$, which were labeled observed and used in the structure refinement. Two rescans were applied for weak reflections. Corrections were made for the Lorentzian and polarization factors. Three standard reflections monitored at every 150 reflections showed an intensity deterioration by 0.7% of the initial value. The falling-off of the intensities with the elapse of time was corrected based on the linear decay in the standard reflections. The structure was solved by direct methods (program used: TEXSAN) and refined by the similar full-matrix least squares procedure with the weighting scheme $\omega = 1/[\sigma^2 (F_0)]$. The positions of the hydrogen atoms were idealized (C−H, 0.95 Å), assigned to isotropic thermal parameters $B(H) = 1.2B_{eq}(C)$, and allowed to ride on their parent carbons.

2.3. Susceptibility Measurement. The paramagnetic susceptibility measurements were carried out with a SQUID magnetometer in the temperature range of 1.8−300 K. The measurements were performed in the magnetic field (*H*) of 0.1T to avoid saturation effects. The susceptibilities of *p*-FPDV, *p*-PyDV, and *m*-PyDV were corrected for the diamagnetic contributions of $\chi_{dia} = -0.196 \times 10^{-3}$, -0.188×10^{-3}, and -0.188×10^{-3} emu/mol, respectively, calculated by Pascal's method.

3. Results

3.1. Crystal Structures. The crystal structure could be determined for the *p*-FPDV radical. Our attempts, however, to determine the crystal structures of the *p*- and *m*-PyDV have as yet been unsuccessful because of the inadequate quality of their crystals. Crystal data obtained for the *p*-FPDV are as follows: orthorhombic, space group $P2_12_12_1$, $a = 18.332(4)$, $b = 21.510(4)$, $c = 4.0443(5)$Å, $V = 1594.7(5)$Å^3, $Z = 4$, and finally $R = 0.059$ using 999 observed reflections with $I > 2.50\sigma(I)$. In Figure 1 we show the molecular structure of *p*-FPDV. The atom numbering scheme and molecular conformation of the verdazyl radical are shown in Figure 1. Figures 2 and 3 show a projection of the structure along the *c*- and *b*-axes, respectively. The *p*-FPDV molecules at (0,0,0) and (0.5,0,0) form one-dimensional (1D) chains, respectively, along the *c*-axis with moderately short $N_i - N_i$ ($i = 1-4$) contacts (4.04 Å) between the nitrogen atoms in the central hydrazidinyl moiety N1−N2−C1−N3−N4. The

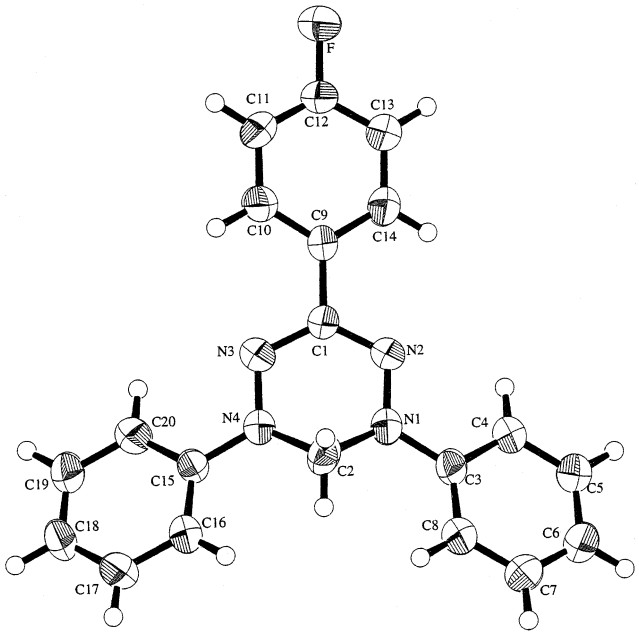

Figure 1. Molecular structure of the *p*-FPDV radical with the atom numbering scheme.

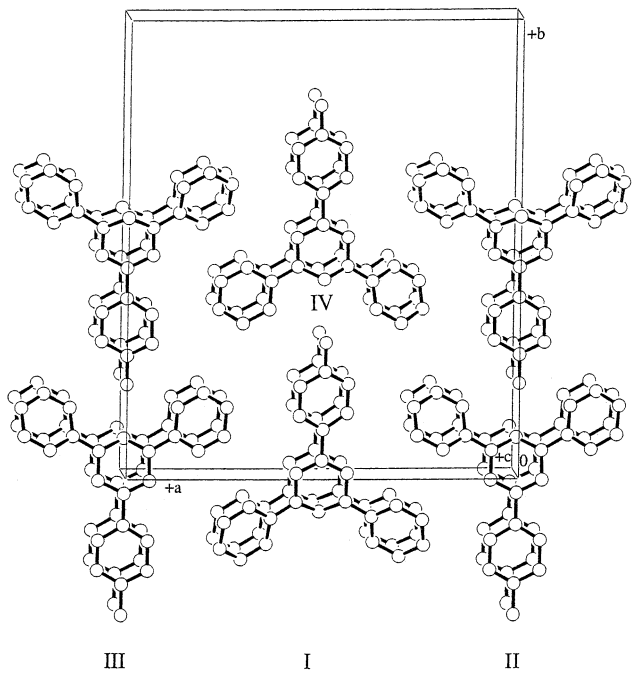

Figure 2. Crystal structure of *p*-FPDV viewed along the direction perpendicular to the *ab* plane.

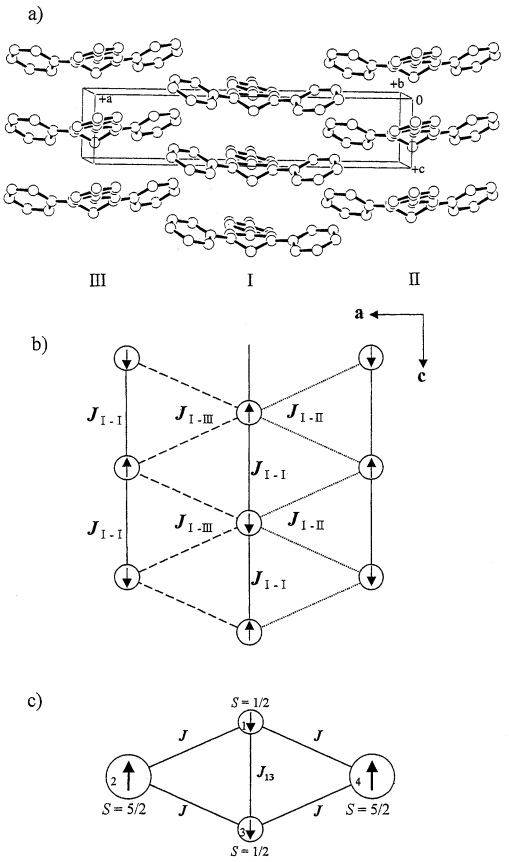

Figure 3. (a) Columnar packing of the *p*-FPDV radical molecules showing the formation of 1D linear-chain along the *c*-axis. (b) The exchange pathways including spin frustration interaction and spin alignment for the ground state of *p*-FPDV. (c) Spin alignment for the ground state of $[Mn(hfac)_2]_2(bnn)$ complex having butterfly-type spin frustration interaction.

TABLE 1: Pertinent Intermolecular Contacts[a] (r_{Ij} (Å)) and the Sign Expected for the Interatomic Exchange Interaction J_{Ij} ($= J_{Ij}^{AB}\rho_i^A\rho_j^B$) in Eq 2

r_{ij} (I−I)	J_{ij}	r_{ij} (I−II)	J_{ij}	r_{ij} (I−III)	J_{ij}	r_{ij} (I−IV)	J_{ij}
F−F 4.04	−	N3−C19 4.02	+	N2−C5 3.84	+	F−N1 3.74	+
N1−N1 4.04	−	C19−C20 3.79	+	C4−C5 3.73	+	F−N4 3.78	+
N1−N2 4.05	−	C20−C19 3.75	+	C5−C4 3.90	+	F−C3 3.67	−
N2−N1 4.47	−	C20−C20 3.84	−	C4−C4 3.83	−	F−C8 3.29	+
N2−N2 4.04	−					F−C15 3.80	−
N3−N3 4.04	−					F−C16 3.46	+
N3−N4 4.45	−						
N4−N3 4.07	−						
N4−N4 4.04	−						

[a] The estimated standard deviations are in the range of 0.005−0.01 Å.

short N−N and N−C distances obtained for four kinds of molecular pairs (I−I, I−II, I−III, and I−IV) are listed in Table 1.

The molecular structure of *p*-FPDV in the crystal is similar to that reported for 1,3,5-triphenylverdazyl (TPV) and other 1,3,5-triarylverdazyls.[12,17,30,31] The data of the central hydrazidinyl moiety N1−N2−C1−N3−N4 (N1−N2 1.352(8) Å and N3−N4 1.346(8)Å, N2−C1 1.322(7) Å and N3−C1 1.342(7)Å; N1−N2−C1 114.8(5)°, N2−C1−N3 127.2(4)°) are similar to mean data of 1,3,5-triphenylverdazyl: N1−N2 1.351(3) Å, N2−C1 1.338(1) Å; N1−N2−C1 114.4(2)°, N2−C1−N3 126.8°, and to those of other 1,3,5-triarylverdazyls. As in these compounds, the four nitrogens of the verdazyl ring in *p*-FPDV are nearly planar, and the verdazyl ring has an unsymmetrical boat conformation, with both C1 and C2 being out of the nitrogen plane on the same side. C1 is displaced by only +0.078(10) Å, while C2 is displaced by +0.576(10) Å. The interplanar angle between the N1−N2−N3−N4 and C3−C4−C5−C6−C7−C8 planes is 22.8(3)°, between the N1−N2−N3−N4 and C9−C10−C11−C12−C13−C14 planes 12.2(2)°, and between the N1−N2−N3−N4 and C15−C16−C17−C18−C19−C20 planes 23.7(3)°.

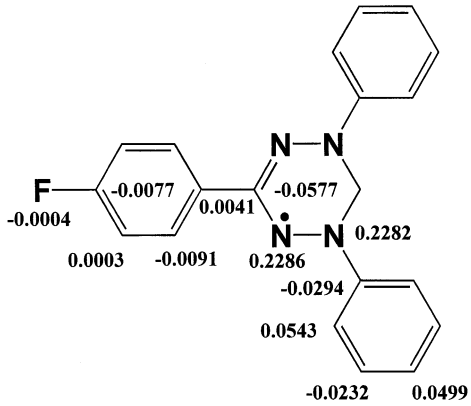

Figure 4. McLachlan unpaired spin densities on the *p*-FPDV radical molecule.

3.2. Unpaired Spin Distributions on the *p*-FPDV, *p*-PyDV, and *m*-PyDV Radical Molecules. The McLachlan spin densities (ρ_i) of the *p*-FPDV radical were calculated by using the following MO parameters:[32] $\alpha_{N1} = \alpha_{N4} = \alpha + 1.2\beta$, $\alpha_{N2} = \alpha_{N3} = \alpha + 1.0\beta$, $\beta_{C-N} = 1.2\beta$, $\beta_{N-N} = 1.0\beta$ for the nitrogen atom of the verdazyl ring and $\alpha_F = \alpha + 3.0\beta$, $\beta_{C-F} = 0.7\beta$ for the fluorine atom. The resonance integral $\beta_{C1-C(ph)} = \beta \cos 12°$, $\beta_{N1-C(ph)} = \beta_{N4-C(ph)} = \beta \cos 23°$, where the choice of θ_i was made on the basis of the results of the X-ray analysis of the *p*-FPDV radical crystal (see Supporting Information). The McLachlan MO parameter λ was given the standard value of 1.2. The McLachlan spin densities (ρ_i) of *p*-FPDV calculated with these parameters are given in Figure 4.

Similarly, the unpaired spin densities were calculated for the *p*-PyDV and *m*-PyDV radicals. The unpaired spin densities obtained (data are not shown) are very similar to those of *p*-FPDV. The singly occupied molecular orbitals (SOMO) containing an unpaired electron of the *p*-FPDV, *p*-PyDV, and *m*-PyDV radicals have, at least in the Hückel approximation, a node in the C1-phenyl ring and a C1 carbon atom connected to the phenyl ring, giving a zero spin density on the C1-phenyl ring. In the McLachlan approximation, the orbitals are spin-polarized so as to yield nonvanishing spin densities in the C1-phenyl ring of the radical. However, the unpaired spin densities on the C1-phenyl ring are very small, as shown in Figure 4.

The unpaired spin distributions ($\Sigma\rho_i$) on the central verdazyl, N1- (and N4-) phenyl, and C1-phenyl rings are $\Sigma\rho_i$ (verdazyl) = 0.8559, $\Sigma\rho_i$ (N1- (and N4-) phenyl) = 0.0827, and $\Sigma\rho_i$ (C1-phenyl) = −0.0216, respectively. About 86% of unpaired spin density distributes on the central verdazyl ring including four nitrogen atoms. The spin density on the C1-phenyl ring is smaller than those on the central verdazyl and N1- (and N4-) phenyl rings, as expected. Similarly, for *p*-PyDV, $\Sigma\rho_i$ (verdazyl) = 0.8564, $\Sigma\rho_i$ (N1- (and N4-) phenyl) = 0.0836, and $\Sigma\rho_i$ (C1-phenyl) = −0.0233, and, for *m*-PyDV, $\Sigma\rho_i$ (verdazyl) = 0.8556, $\Sigma\rho_i$ (N1- (and N4-) phenyl) = 0.0830, and $\Sigma\rho_i$ (C1-phenyl) = −0.0217. The results of McLachlan MO calculations show that there are large positive and negative atomic π-spin densities in the central verdazyl and N1-(and N4-)phenyl rings. As described later, this situation is one of the important requirements for the

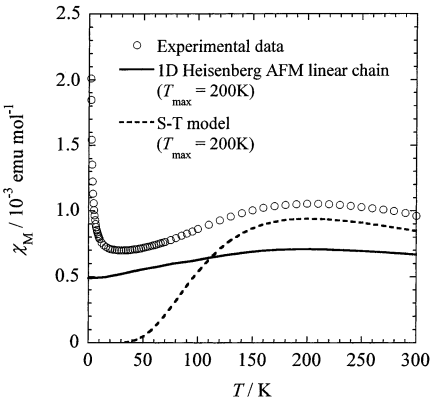

Figure 5. Temperature dependence of the magnetic susceptibility (χ_M) (○) of the *p*-FPDV radical crystal. The solid (—) and dashed (- - -) curves are the theoretical susceptibilities calculated for the 1D AFM Heisenberg linear-chain model ($\alpha = J_2/J_1 = 1$) and S−T equilibrium model ($\alpha = 0$) with $T_{max} = 200$ K, respectively.

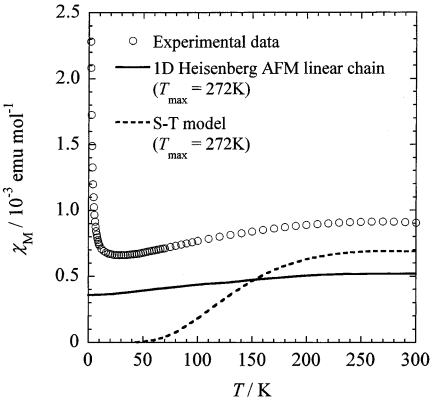

Figure 6. Temperature dependence of the magnetic susceptibility (χ_M) (○) of the *p*-PyDV radical crystal. The solid (—) and dashed (- - -) curves are the theoretical susceptibilities calculated for the 1D AFM linear-chain model ($\alpha = J_2/J_1 = 1$) and S−T equilibrium model ($\alpha = 0$) with $T_{max} = 272$ K, respectively.

intermolecular FM exchange interaction in organic radical crystals.[4,33−35]

3.3. Magnetic Susceptibilities of *p*-FPDV, *p*-PyDV, and *m*-PyDV Radical Crystals. The magnetic susceptibility, χ_M, obtained for *p*-FPDV is shown in Figure 5 as a function of temperature. When the temperature is lowered from 300 K, χ_M increases gradually and reaches a broad maximum at $T_{max} = 200 \pm 10$ K. After passing through the maximum, χ_M decreases gradually down to 30 K. Below 10 K, χ_M increases abruptly as the temperature is lowered.

To ascertain whether the abrupt increase of susceptibility below 10 K is due to the weak ferromagnetic transition or not, the magnetization measurements have been performed at 1.8 K. At 1.8 K the remanence was not observed and the magnetization was almost proportional to the magnetic field up to 1 T (data are not shown), indicating that the abrupt increase of susceptibility below 10 K is due to the Curie impurity. The residual paramagnetic radical concentration, calculated from the susceptibility at 1.8 K and assuming validity of the Curie law, is only about 0.6%.

Similar magnetic behavior was observed for *p*-PyDV and *m*-PyDV radical crystals, showing a broad maximum at $T_{max} =$ 272 and 157 K, respectively, as shown in Figures 6 and 7. The Curie impurities calculated are 0.8 and 0.7%, respectively.

The values of T_{max} observed for *p*-FPDV (200 K), *p*-PyDV (272 K), and *m*-PyDV (157 K) are 1 or 2 orders of magnitude

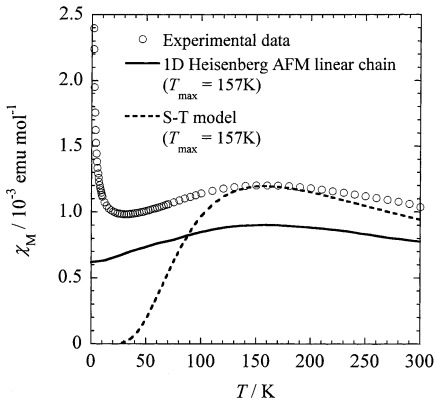

Figure 7. Temperature dependence of the magnetic susceptibility (χ_M) (○) of the *m*-PyDV radical crystal. The solid (—) and dashed (- - -) curves are the theoretical susceptibilities calculated for the 1D AFM linear-chain model ($\chi = J_2/J_1 = 1$) and S−T equilibrium model ($\alpha = 0$) with $T_{max} = 157$ K, respectively.

larger than those for usual organic neutral radical crystals, indicating strong intermolecular AFM exchange interaction (J). As far as we know, these are the largest values of T_{max} found for usual organic neutral radical crystals including verdazyl type free radical solids.

4. Discussion

4.1. Anomalous Magnetic Behavior in *p*-FPDV, *p*-PyDV, and *m*-PyDV. The χ_M of the *p*-FPDV, *p*-PyDV, and *m*-PyDV shows a broad maximum. Such a magnetic behavior is characteristic of a 1D Heisenberg AFM substance. Therefore, the susceptibilities of *p*-FPDV, *p*-PyDV, and *m*-PyDV were compared with theoretical predictions based on Heisenberg exchange-coupled alternating linear chains.[36,37] The corresponding spin Hamiltonian is given by

$$H = -2J_1\sum_{i=1}^{N/2} S_{2i}S_{2i+1} - 2J_2\sum_{i=1}^{N/2} S_{2i-1}S_{2i} \qquad (1)$$

where J_1 and J_2 are the nearest-neighbor exchange integrals. Negative values of J_1 and J_2 corresponding to AFM coupling are appropriate to the free radicals considered here. The parameter $\alpha(= J_2/J_1)$ conveniently indicates the degree of alternation and $\alpha = 1$ corresponds to the uniform limit, that is, a nonalternating AFM chain. The parameter $\alpha = 0$ corresponds to an isolated dimer (spin-pair) system, and in this case the susceptibility should be interpreted by the singlet−triplet (S−T) equilibrium model.

As described in a previous section, the susceptibilities of the *p*-FPDV, *p*-PyDV, and *m*-PyDV show a broad maximum at $T_{max} = 200$, 272, and 157 K, respectively, and seem to have nonzero χ_M at $T = 0$, which is a characteristic feature of the isotropic 1D Heisenberg nonalternating antiferromagnet. In fact, the result of X-ray crystal analysis shows that the molecules of *p*-FPDV are packed in columns along the *c*-axis and the verdazyl rings with high-spin density overlap each other with comparatively short intermolecular distance (4.04 Å) in the crystal.

Therefore, the observed susceptibility of *p*-FPDV with $T_{max} =$ 200 K was compared with theoretical susceptibillities calculated for the $S = 1/2$ 1D Heisenberg AFM linear-chain model.[36] However, as shown in Figure 5, the susceptibility cannot be explained by the above model with an exchange interaction of $2J/k_B = -1.56T_{max} = -312$ K. The χ_{max}^{obsd} value (1.05×10^{-3} emu/mol) observed is 1.48 times larger than the theoretical value ($\chi_{max}^{1D} = 0.142/T_{max} = 7.10 \times 10^{-4}$ emu/mol) calculated for 1D

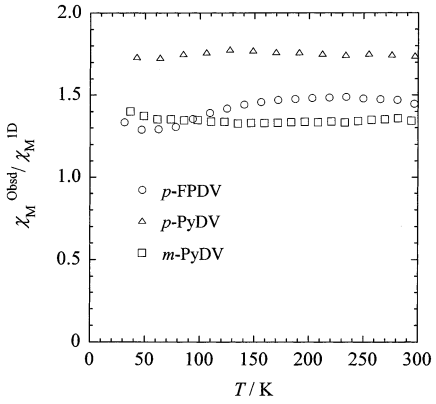

Figure 8. The $\chi_M^{obsd}/\chi_M^{1D}$ vs T plots for the *p*-FPDV, *p*-PyDV, and *m*-PyDV radical crystals.

Heisenberg AFM linear-chain model. Further, the susceptibility cannot be explained by a S−T model, as expected (see Figure 5).

Similarly, the measured susceptibilities of *p*-PyDV and *m*-PyDV with T_{max}= 272 and 157 K, respectively, were compared with theoretical susceptibilities calculated for the 1D Heisenberg AFM linear-chain model.[36] As shown in Figures 6 and 7, the susceptibility−temperature data (open circles) for *p*-PyDV and *m*-PyDV are different from theoretical values (solid curve); for instance, the experimental values of the susceptibility ($\chi_{max}^{obsd} = 9.12 \times 10^{-4}$ and 11.99×10^{-4} emu/mol) at $T_{max} =$ 272 and 157 K are 1.75 and 1.33 times larger than the theoretical values ($\chi_{max}^{1D} = 0.142/T_{max} = 5.22 \times 10^{-4}$ and 9.04×10^{-4} emu/mol) for *p*-PyDV and *m*-PyDV, respectively. The $\chi_M^{obsd}/\chi_M^{1D}$ vs T plots are shown in Figure 8. The ratios are 1.42 ± 0.13, 1.76 ± 0.06, and 1.35 ± 0.05 for *p*-FPDV, *p*-PyDV, and *m*-PyDV, respectively, and are nearly temperature-independent. As shown in Figures 6 and 7, the S−T model also cannot explain the magnetic properties of these radical crystals.

4.2. Existence of Frustrated Ferromagnetic Spin Interaction in the System. The sign and magnitude of the exchange interaction between the π-electron spins may be conjectured on the basis of the spin densities and the molecular packing. For the exchange interaction of conjugated π-spin radicals, such as verdazyl radical being considered, the following two-spin Hamiltonian proposed by McConnell[33] is certainly useful:

$$H^{AB} = -2\boldsymbol{S}^{A}\cdot\boldsymbol{S}^{B}\Sigma\, J_{ij}^{AB}\rho_i^{A}\beta_j^{B} \qquad (2)$$

where $\boldsymbol{S}^A$ and $\boldsymbol{S}^B$ are the total spins on the A and B molecules and where ρ_i^A and ρ_j^B are the π-spin densities on the i and j atoms of A and B molecules, respectively. The exchange integral, J_{ij}^{AB}, depends on the overlap integral between the $2p_z\pi$ orbitals of the i and j atoms, and is certainly negative for all the interatomic contacts in the present case, although we cannot estimate its precise magnitude at present. Consequently, the sign of the resulting exchange interaction between the ith and jth atoms is dependent on the sign of the spin density product of $\rho_i^A\rho_j^B$.[4,34,35]

The result of McLachlan MO calculations shows that there are large positive and negative atomic π-spin densities in the central verdazyl and N1-(and N4-)phenyl rings, and it is quite possible that, in special cases, these radicals may interact to each other in the crystal lattice so that atoms of a positive spin density are exchange-coupled most strongly to atoms of a negative spin density in neighboring molecules. In such a case, the apparent exchange interaction is ferromagnetic, corresponding to the results verified experimentally by magnetic susceptibility measurements of the 3-(4-nitrophenyl)-1,5,6-triphenylverdazyl (NPTV) radical crystal.[38] NPTV was found to be an antiferromagnet with a Neel temperature of $T_N = 1.16 \pm 0.04$ K. Above the transition temperature T_N, NPTV behaves as a quasi-one-dimensional Heisenberg ferromagnet with the intrachain exchange interaction of $2J/k_B = +7.0 \pm 1.0$ K.[12] In this structure the verdazyl ring with large positive spin populations at the nitrogens is in contact with the adjacent coplanar 4-nitrophenyl segment bearing small positive and negative spin populations. Many examples of quasi-1D Heisenberg ferromagnet were observed for the other verdazyl radical crystals.[7−10,12−14]

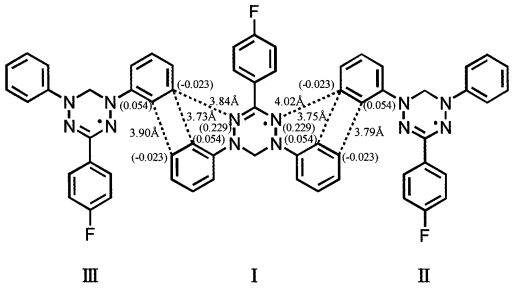

Figure 9. View perpendicular to the *ab* plane showing the interatomic distances between the *p*-FPDV radical molecules and unpaired spin densities.

As described above, the crystal structure of *p*-FPDV radical crystal shows a particular one-dimensional arrangement of the verdazyl moieties (Figures 2 and 3). The molecules of *p*-FPDV are packed in columns along the *c*-axis. Within the array, the central verdazyl ring with large positive spin distributions at the four nitrogens and the verdazyl ring of adjacent verdazyl molecules lie parallel to each other, and the interplane distance is 4.04 Å, which corresponds to the lattice constant of *c*-axis. The result suggests strong AFM intrachain interaction (J_{I-I}) along the *c*-axis, giving large T_{max} (= 200 K) value.

As shown in Figures 2 and 3, the 1D *p*-FPDV chain I overlaps with two sides of 1D *p*-FPDV chain II and chain III, resulting in the two-dimensional (2D) chain formation within the *ac* plane. As shown in Figure 9 and as listed in Table 1, there are several close contacts between the atoms with positive spin density in molecule I and the atoms with negative spin density in molecule II and in molecule III. These contacts will contribute to the FM interaction, because $J_{ij}^{AB}\rho_i^A\rho_j^B$ in eq 2 is positive. Only the C20−C20 contact in the molecular pair I−II and C4−C4 contact in the pair I−III will contribute to AFM interaction. As a result, we can expect two kinds of FM interactions ($J_{I-II} > 0$ and $J_{I-III} > 0$) between 1D AFM *p*-FPDV chains.

As can be seen from Figure 2 and as listed in Table 1, the close contact occurs between the fluorine atom F of molecule I and the carbon and nitrogen atoms in the molecule IV along the *b*-axis. However, this contact (J_{I-IV}) along the *b*-axis is considered to be negligible, because the spin density distribution ($\Sigma\rho_i = -0.0216$) on the 1-(fluorophenyl) ring is very small, and especially ρ_F is −0.0004. As a result, *p*-FPDV molecules form 2D magnetic lattice in a crystal.

On the other hand, as shown in Figure 3, the unpaired spin on *p*-FPDV molecules that form the 1D *p*-FPDV chain I interacts magnetically with the right-hand side spin on the *p*-FPDV molecule of 1D chain II through two bonds with the same FM exchange interaction (J_{I-II}). For such an interaction we can expect spin frustration. The spin frustration may arise from the topology of the magnetic sites, and this is the case for the isosceles triangles, which is a typical situation of frustrated spin interactions. One of the possible spin arrangements within the *ac*-plane is shown in Figure 3b. Similarly, the spin on the

p-FPDV molecule in the chain I interacts with the left-hand side spin on *p*-FPDV molecule of 1D chain III through two bonds with the same FM exchange interaction (J_{I-III}), where J_{I-III} is similar to J_{I-II}, but is not equal to J_{I-II}.

In *p*-FPDV, if the absolute value of J_{I-I} is much larger than those of J_{I-II} and J_{I-III}, the susceptibility will be explained by a simple 1D Heisenberg AFM linear-chain model. Inversely, if the $|J_{I-II}|$ and $|J_{I-III}| \gg |J_{I-I}|$, the 2D network sheet connected with FM interactions (J_{I-II} and J_{I-III}) will be formed within the *ac*-plane. The result of the susceptibility measurement of *p*-FPDV does not correspond to the above two cases. Consequently, we have to consider the case of four spin system, that is, butterfly-type spin frustration, as described below. As shown in Figure 3b, only the J_{I-I} is negative among five interactions included in the butterfly type four spin system.

Spin frustration is one of the interesting magnetic behaviors.[24] However, the examples of the frustrated systems that have been experimentally studied so far are almost limited to inorganic compounds. The examples of real organic spin frustration compounds are very limited.[25−28] Awaga et al.[25] studied the structural and magnetic properties of the (*m*-MPYNN)$^+$·$(ClO_4^-)_x$·$(I^-)_{1-x}$·1/3(acetone) ($0 \le x \le 1$) (*m*-MPYNN = *m*-*N*-methylpyridinium α-nitronyl nitroxide) system, and found that this system can be characterized as a spin-1 *kagome* antiferromagnet. The Heisenberg *kagome* antiferromagnet is well known as one of the most interesting examples of the frustrated systems.[39] The example of the spin frustration compound was also reported for the BDPA·benzene radical crystal (BDPA = 1,3-bisdiphenylene-2-phenyl-allyl), showing the possibility of the isosceles triangle type spin frustration in the system.[26] Further, the example of an isosceles triangular three spin system with negative *J*'s that would show spin frustration is reported for the organic nitroxide triradical, that is, 2,4-dimethoxy-1,3,5-benzenetriyltris(*N*-*tert*-butyl nitroxide).[27]

A new spin-frustrated system consisting of [Mn(hfac)$_2$] (manganese (II) bis(hexafluoroacetylacetone)) and *bnn* (2,2′-bis(1-oxyl-3-oxide-4,4,5,5-tetramethyl-imidazolinyl, that is, bis-(nitronyl nitroxide)) has been reported by Tanaka et al.[28] This heterospin system displays butterfly-type spin frustration between two organic radical molecules ($S = 1/2$) and two transition metal ions ($S = 5/2$), as shown in Figure 3c. In this four spin system, the large AFM interaction (J_{13}) was made ineffective by the butterfly spin configuration. Although J_{13} is more negative than *J*, the latter wing-body AFM interaction (*J*) is dominated, and the two $S = 1/2$ spins of the *bnn* moiety are obliged to align in parallel. The butterfly configuration and two $S = 5/2$ spins of the manganese ions at the wing sites therefore play an important role in dictating this spin configuration.

As described above, the exchange pathway observed for the *p*-FPDV system seems to be similar to that for the [Mn(hfac)$_2$]-(*bnn*) system, although all the spins are $S = 1/2$, wing-body interactions (J_{I-II} and J_{I-III}) are ferromagnetic, and butterfly-type frustration spreads out the whole 2D network sheet in the former. If the FM interchain interactions (J_{I-II} and J_{I-III}) are not weak and comparable to AFM intrachain interaction (J_{I-I}), all the spins in the butterfly spin system will prefer to take a parallel conformation. As a result, the magnetic moments are enhanced and the susceptibility will increase by about 42% at all the temperature regions. The ratio ($\chi_M^{obsd}/\chi_M^{1D}$) will depend on both the ratios ($|J_{I-II}|/|J_{I-I}|$ and $|J_{I-III}|/|J_{I-I}|$) in the crystals.

p- and *m*-PyDV showed magnetic properties similar to that of *p*-FPDV. The unpaired spin distributions of *p*- and *m*-PyDV radical molecules are similar to that of the *p*-FPDV, as the results of McLachlan MO calculation indicate. Consequently, we can expect similar magnetic structure, that is, the existence of spin frustration in these radical crystals. However, we have not succeeded in preparing single crystals of these radicals. To discuss the details of the origin of anomalous magnetic properties observed for the *p*-PyDV and *m*-PyDV radical crystals, the information about the crystal structures of the verdazyl radicals is necessary.

5. Summary

Anomalous magnetic properties have been observed for three kinds of verdazyl radical crystals (*p*-FPDV, *p*-PyDV, and *m*-PyDV). The magnetic susceptibilities of these radicals show a broad maximum at $T_{max} = 200$, 272, and 157 K, respectively. However, the susceptibility cannot be explained by the 1D Heisenberg AFM linear- and alternating-chain models, which can be generally used for the analyses of the magnetic property of the usual organic radical crystals. The susceptibilities of the *p*-FPDV, *p*-PyDV, and *m*-PyDV are about 42, 76, and 35% larger than the corresponding susceptibilities calculated by a 1D Heisenberg AFM linear-chain model at the temperature region (30−300 K), respectively. The results of the X-ray structure analysis and unpaired spin density calculation of the *p*-FPDV radical indicate that *p*-FPDV radical molecules form a 2D magnetic network that includes a strong AFM intrachain interaction (J_{I-I}) and two kinds of FM interchain interactions (J_{I-II} and J_{I-III}), forming a butterfly-type spin frustration system. The increase of the susceptibilities may be explained by the spin frustration including FM interchain interactions in the *p*-FPDV radical crystals.

Acknowledgment. We are very grateful to Professor F. A. Neugebauer for his kind help for the synthesis of the *p*-FPDV radical crystal. We are also grateful to Mr. Y. Shimobe for the syntheses of the *p*- and *m*-PyDV radical crystals. This work was partly supported by the Grant-in-Aid for Scientific Research, No. 08454225, from the Ministry of Education, Science and Culture, Japan. This work was also partly supported by the Grant-in-Aid for Scientific Research on Priority Areas (B) of Molecular Conductors and Magnets (Area No. 730/11224205) from the Ministry of Education, Science, Sports and Culture, Japan. This work was supported by the Joint Studies Program (2000−2001) of the Institute for Molecular Science.

Supporting Information Available: Tables listing detailed crystallographic data, atomic positional parameters, and bond lengths and angles. This material is available free of charge via the Internet at http://pubs.acs.org.

References and Notes

(1) Tamura, M.; Nakazawa, Y.; Shiomi, D.; Nozawa, K.; Hosokoshi, Y.; Ishikawa, M.; Takahashi, M.; Kinoshita, M. *Chem. Phys. Lett*. **1991**, *186*, 401.

(2) Nakazawa, Y.; Tamura, M.; Shirakawa, N.; Shiomi, D.; Takahashi, M.; Kinoshita, M.; Ishikawa, M. *Phys. Rev*. **1992**, *B46*, 8906.

(3) Kinoshita, M. *Jpn. J. Appl. Phys*. **1994**, *33*, 5718, and references therein.

(4) Azuma, N. *Bull. Chem. Soc. Jpn*. **1982**, *55*, 1357, and references therein.

(5) Kremer, R. K.; Kanellakopulos, B.; Bele, P.; Brunner, H.; Neugebauer, F. A. *Chem. Phys. Lett*. **1994**, *230*, 255.

(6) Tomiyoshi, S.; Yano, T.; Azuma, N.; Shoga, M.; Yamada, K.; Yamauchi, J. *Phys. Rev*. B **1994**, *49*, 16031.

(7) Mukai, K.; Kawasaki, S.; Jamali, J. B.; Achiwa, N. *Chem. Phys. Lett*. **1995**, *241*, 618.

(8) Takeda, K.; Konishi, K.; Nedachi, K.; Mukai, K. *Phys. Rev. Lett*. **1995**, *74*, 1673.

(9) Takeda, K.; Hamano, T.; Kawae, T.; Hidaka, M.; Takahashi, M.; Kawasaki, S.; Mukai, K. *J. Phys. Soc. Jpn*. **1995**, *64*, 2343.

(10) Mukai, K.; Konishi, K.; Nedachi, K.; Takeda, K. *J. Phys. Chem*. **1996**, *100*, 9658.
(11) Mito, M.; Nakano, H.; Kawae, T.; Hitaka, M.; Takagi, S.; Deguchi, H.; Suzuki, K.; Mukai, K.; Takeda, K. *J. Phys. Soc. Jpn.* **1997**, *66*, 2147.
(12) Mito, M.; Takeda, K.; Mukai, K.; Azuma, N.; Gleiter, M. R.; Krieger, C.; Neugebauer, F. A. *J. Phys. Chem*. **1997**, *101*, 9517.
(13) Mukai, K.; Nuwa, M.; Morishita, T.; Muramatsu, T.; Kobayashi, T. C.; Amaya, K. *Chem. Phys. Lett.* **1997**, *272*, 501.
(14) Mukai, K.; Nuwa, M.; Suzuki, K.; Nagaoka, S.; Achiwa, N.; Jamali, J. B. *J. Phys. Chem.* B **1998**, *102*, 782.
(15) Mukai, K.; Shimobe, Y.; Jamali, J. B.; Achiwa, N. *J. Phys. Chem*. B **1999**, *103*, 10876.
(16) Hicks, R. G.; Lemaire, M. T.; Ohrstrom, L.; Richardson, J. F.; Thompson, L. K.; Xu, Z. *J. Am. Chem. Soc.* **2001**, *123*, 7154.
(17) Williams, D. E. *Acta Crystallogr*. B **1975**, *29*, 96.
(18) Neugebauer, F. A.; Fisher H.; Krieger, C. *J. Chem. Soc., Perkin Trans.* 2 **1993**, 535.
(19) Mukai, K.; Jinno, S.; Shimobe, Y.; Azuma, N.; Hosokoshi, Y.; Inoue, K.; Taniguchi, M.; Misaki, Y.; Tanaka, K. *Polyhedron* **2001**, *20*, 1537.
(20) Nakatsuji, S.; Kitamura, A.; Takai, A.; Nishikawa, K.; Morimoto, Y.; Yasuoka, N.; Kawamura, H.; Anzai, H. *Z. Naturforsch.* **1998**, *53b*, 495.
(21) Brook, D. J. R.; Lynch, V.; Conklin, B.; Fox, M. A. *J. Am. Chem. Soc.* **1997**, *119*, 5155.
(22) Brook, D. J. R.; Fornell, S.; Stevens, J. E.; Noll, B.; Kock, T. H.; Eisfeld, W. *Inorg. Chem.* **2000**, *39*, 562.
(23) Hicks, R. G.; Lemaire, M. T.; Thompson, L. K.; Barclay, T. M. *J. Am. Chem. Soc.* **2000**, *122*, 8077.
(24) Fazekas, P.; Anderson, P. W. *Philos. Mag.* **1974**, *30*, 423.
(25) Awaga, K.; Okuno, T,; Yamaguchi, A.; Hasegawa, M.; Inabe, T.; Maruyama, Y.; Wada, N. *Phys. Rev.* B **1994**, *49*, 3795.
(26) Azuma, N.; Ozawa, T.; Yamauchi, J. *Bull. Chem. Soc. Jpn.* **1994**, *67*, 31.
(27) Fujita, J.; Tanaka, M.; Suemune, H.; Koga, N.; Matsuda, K.; Iwamura, H. *J. Am. Chem. Soc.* **1996**, *118*, 9347.
(28) Tanaka, M.; Matsuda, K.; Itoh, T.; Iwamura, H. *Angew. Chem., Int. Ed. Engl*. **1998**, *37*, 810.
(29) Kuhn, R.; Neugebauer, F. A.; Trischmann. H. *Angew. Chem.* **1964**, *76*, 691.
(30) Azuma, N.; Deguchi, Y.; Marumo, F.; Saito, Y. *Bull. Chem. Soc. Jpn.* **1975**, *48*, 819.
(31) Azuma, N.; Deguchi, Y.; Marumo, F.; Saito, Y. *Bull. Chem. Soc. Jpn.* **1975**, *48*, 825.
(32) Fischer, H. H. *Tetrahedron* **1967**, *23*, 1939.
(33) McConnell, H. M. *J. Chem. Phys.* **1963**, *39*, 1910.
(34) Azuma, A.; Yamauchi, J.; Mukai, K.; Ohya-Nishiguchi, H.; Deguchi, Y. *Bull. Chem. Soc. Jpn.* **1973**, *46*, 2728.
(35) Izuoka, A.; Murata, S.; Sugawara, T.; Iwamura, H. *J. Am. Chem. Soc.* **1987**, *109*, 2631.
(36) Bonner, J. C.; Fisher, M. E. *Phys. Rev.* **1964**, *A135*, 640.
(37) Bonner, J. C.; Blote, H. W. J.; Bray, J. W.; Jacobs, I. S. *J. Appl. Phys*. **1979**, *50*, 1810.
(38) Allemand, P.-M.; Srdanov, G.; Wudl, F. *J. Am. Chem. Soc.* **1990**, *112*, 9391.
(39) Syozi, I. *Prog. Theor. Phys.* **1951**, *6*, 306.